

Alma Mater Studiorum Università di Bologna  
Archivio istituzionale della ricerca

An Ambient-Insensitive Battery-Less Wireless Node for Simultaneous Powering and Communication

This is the final peer-reviewed author's accepted manuscript (postprint) of the following publication:

*Published Version:*

G. Paolini, D.M. (2021). An Ambient-Insensitive Battery-Less Wireless Node for Simultaneous Powering and Communication. Institute of Electrical and Electronics Engineers Inc. [10.23919/EuMC48046.2021.9338073].

*Availability:*

This version is available at: <https://hdl.handle.net/11585/794323> since: 2023-11-24

*Published:*

DOI: <http://doi.org/10.23919/EuMC48046.2021.9338073>

*Terms of use:*

Some rights reserved. The terms and conditions for the reuse of this version of the manuscript are specified in the publishing policy. For all terms of use and more information see the publisher's website.

This item was downloaded from IRIS Università di Bologna (<https://cris.unibo.it/>).  
When citing, please refer to the published version.

(Article begins on next page)

This is the final peer-reviewed accepted manuscript of:

**G. Paolini, D. Masotti, M. Guermandi, M. Shanawani, L. Benini and A. Costanzo, "An Ambient-Insensitive Battery-Less Wireless Node for Simultaneous Powering and Communication," *2020 50th European Microwave Conference (EuMC)*, Utrecht, Netherlands, 2021, pp. 522-525**

The final published version is available online at:

<https://doi.org/10.23919/EuMC48046.2021.9338073>

#### Terms of use:

Some rights reserved. The terms and conditions for the reuse of this version of the manuscript are specified in the publishing policy. For all terms of use and more information see the publisher's website.

*This item was downloaded from IRIS Università di Bologna (<https://cris.unibo.it/>)*

***When citing, please refer to the published version.***

# An Ambient-Insensitive Battery-Less Wireless Node for Simultaneous Powering and Communication

G. Paolini<sup>#1</sup>, D. Masotti<sup>#2</sup>, M. Guermandi<sup>#3</sup>, M. Shanawani<sup>#4</sup>, L. Benini<sup>#5</sup>, A. Costanzo<sup>#6</sup>

<sup>#</sup>DEI “Guglielmo Marconi”, University of Bologna, Bologna, Italy

{<sup>1</sup>giacomo.paolini4, <sup>2</sup>diego.masotti, <sup>3</sup>marco.guermandi, <sup>4</sup>mazen.shanawani, <sup>5</sup>luca.benini, <sup>6</sup>alessandra.costanzo}@unibo.it

**Abstract** — This work proposes a new multi-layer architecture for a compact, battery-less sensor node specifically designed to be robust and functional in environments hostile to the electromagnetic propagation, as is the case of the automotive and the industrial sectors. The goal is to enable real time monitoring of difficult-to-be-reached engine parts, to prevent and/or register possible malfunctioning, failure or unwanted warming of the tagged components. In order to enable simultaneous powering and communication, the LoRa (Long Range) protocol has been adopted in the 2.4 GHz frequency band and a RF power source has been used in the same band. A miniaturized, high-efficiency rectenna, designed to be directly in contact with the metallic parts, is used in combination with a power management unit to enable cold-start operations of the sensor. Measurements conducted inside a car engine show that the node is activated in less than 300 seconds with a RF power source located at 54-cm distance.

**Keywords** — Simultaneous Wireless Information and Power Transfer (SWIPT), Industrial IoT, Low Power, RFID.

## I. INTRODUCTION

Over the last years, there has been an always increasing interest of both academic and industrial communities on new systems to provide solutions for monitoring engine components with in-situ sensors [1].

One of the main challenges for the diffusion of this Industrial IoT paradigm, especially in the automotive and robotic sectors, is the reliability of real-time sensing of distributed mechanical parts, possibly rotating and moving, and located in unhandy positions. Currently, such operations are partially possible but are carried out using wired interconnections and are often impossible when the objects to be monitored are moving or difficult to be accessed, and a wireless version has been searched intensively. One of the main issues is the hostile environment for wireless operations, affected by shielding, unpredictable destructive (or constructive) interferences. Indeed, when metallic objects with complex and variable geometries are present, they can compromise a wireless monitoring system reliability. In Fig. 1, an illustrative example of the envisioned scenario is represented.

At the moment, there are no general-purpose solutions available in this field, although several have been presented for specific application scenarios exploiting low-power RFID technology for data communication [2] and metal-compatible customized antennas [3]; miniaturization is another significant constraint as addressed in [4], [5]. Moreover, a WPT system

for automotive application has been presented in [6], with a patch antenna used as transmitter and a dipole or a patch as receiver, but without including a specific power management unit or a dedicated sensing technology.

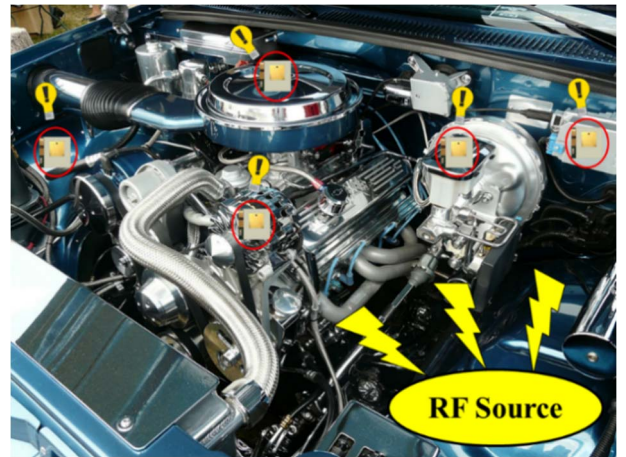


Fig. 1. Envisioned scenario for the exploitation of the proposed battery-less sensor nodes, including a RF source for remote powering.

However, energy autonomy is not guaranteed for the entire system operations, when a significant amount of data must be transferred for communication and sensing purposes.

This work proposes an autonomous wireless node that overcomes the abovementioned limitations. The sensor node is designed as a whole leading to a novel and compact 3-D architecture able to embed the radiative part, the radiofrequency circuits and the baseband power management unit (PMU). The multilayer organization, with the radiative part located on the top layer and decoupled from the rest of the system by a ground plane, ensures highly efficient energy harvesting operation and data communication in a volume as small as 3.8 cm<sup>3</sup>. The low-power LoRa protocol is used for communication via a dedicated chip antenna (characterized by a very small form factor, but rather limited radiation efficiency) co-located with a patch-like antenna (exploiting shorting pins technology for miniaturization while preserving a high radiation efficiency).

Thanks to a frequency division approach, the system is free to communicate while it is charged without interference between the two activities.

## II. DESIGN OF THE WIRELESSLY ACTIVATED NODE

The 3-D implementation of the whole tag has been conceived with the twofold goal of miniaturization and insulation from the metallic environment. The top layer consists of the radiating elements designed to include a metal plate, while the bottom layer hosts the RF rectifier, the radio and the baseband subsystem for power managing purposes, except for two energy storage capacitors that are located on the top layer in order to reduce the overall node thickness.

### A. Top Layer Radiative Part for Wireless Energy and Data Transfer

The radiating part is shown in Fig. 2 and is located on the top layer. It operates in the 2.4 GHz band, for both communication and powering, and consists of two separate antennas, to allow simultaneous wireless powering and information transfer, and to avoid the excess energy consumption of a RF switch, that degrades the energy harvesting operations.

For energy harvesting, a patch antenna miniaturized by means of shorting pins (Fig. 2) has been designed. To reduce the overall node dimensions, a coaxial-feeding technique has been chosen to connect the antenna to the rectifier circuit, which is located on the bottom layer together with the rest of the system circuitry. Using the Rogers RO4350B (thickness: 3.048 mm,  $\epsilon_r=3.48$ ,  $\tan(\delta)=0.0037$ ) and the shorting pins technique, the antenna dimensions, including the substrate, are  $2.50 \times 3.00 \times 0.32$  cm<sup>3</sup>, with a realized gain as high as 1.84 dB, Half Power Beam Width (HPBW) of 116°, radiation efficiency of 74%, and bandwidth (-10 dB) of 35 MHz. These performances have been predicted and measured despite of about 50% antenna size reduction.

The communication operations are carried out by means of the Semtech SX1280 transceiver in the 2.4 GHz ISM (Industrial, Scientific and Medical) band.

Owing to the high sensitivity of the adopted transceiver (down to -132 dBm) working with the LoRa communication protocol, and the need for minimum node dimensions, a commercial chip antenna, specific for on-metal purposes, has been chosen for the communication task (Johanson 2450AT42E0100, dimensions:  $2 \times 5$  mm<sup>2</sup>, thickness: 1.5 mm). On the left side of the patch antenna substrate, an inset of 3.2 mm has been dug, in order to host the chip antenna without increasing the overall node thickness.

Mutual decoupling between the two co-located antennas placed in the same plane has been checked by measurements and is shown in Fig. 3 in terms of the transmittance parameter ( $S_{21}$ ) of the resulting two-port antenna. The plot shows a good isolation (better than 20 dB in the two operating frequencies). The patch antenna reflection coefficient ( $S_{11}$ ) has also been tested and is feasible for the purpose of the application.

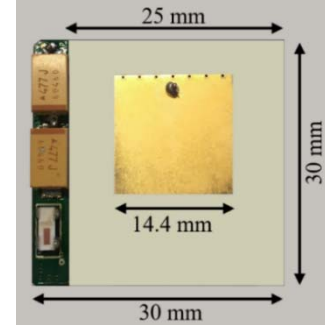


Fig. 2. Top layer of the node: the miniaturized patch with the shorted pins for energy harvesting, the metal-mounted chip antenna, and the storage capacitors are represented.

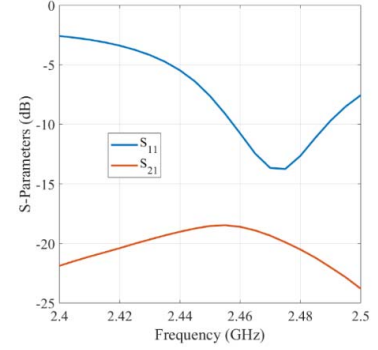


Fig. 3. Measured results of the scattering parameters of the two antennas of the wireless sensor node: port 1 is the port of the patch antenna, whereas port 2 indicates the metal-mounted chip antenna.

### B. Sensor Node for Communication and Power Management Layout

The block schematic of the designed node is shown in Fig. 4, and its circuitual implementation is shown in Fig. 5. It is comprised of: (i) a full-wave rectifier, with a voltage doubler (two Skyworks SMS7630-079LF diodes) and a matching network consisting of one 0.3 pF capacitor and a shorted stub (width: 0.51 mm; length: 5.7 mm), located in the bottom right of Fig. 5, and is connected to the top layer patch antenna port through a via hole (Fig. 2); (ii) a power management section which efficiently controls the energy at the output of the rectifier to charge two 470  $\mu$ F ultra-low leakage tantalum capacitors that allow energy storage on the device and provide power supply to the node; these capacitors are quite thick and have been located on the top layer for 3-D miniaturization of the entire tag; (iii) a low power microcontroller unit (MCU, STMicroelectronics STML32476) to control the node peripherals; (iv) a 2.4 GHz transceiver supporting LoRa communication protocol, feeding a Johanson Technology 2450AT42E0100, a 2.4 GHz SMT above metal mini chip antenna; (v) an ultra-low-power 3-axis accelerometer (STMicroelectronics IIS2DLPC) for inertial sensing; (vi) an ultra-low-power Real Time Clock (RTC, Abracon AB1805) for duty-cycling the node operation by turning on the node at specific time intervals.

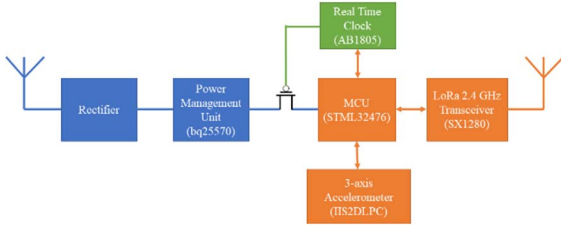


Fig. 4. Block diagram of the wireless sensor node.

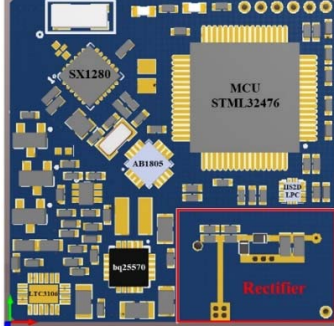


Fig. 5. Bottom layer of the node, with highlighted the main components and the RF-to-DC rectifier.

The node mostly operates in four phases (Fig. 6):

**START-UP:** when the rectified power is available at the PMU input, but the energy storage capacitors are depleted, the node will be forced off by an undervoltage lockout circuit till the storage elements get charged up to 2 V. Only charging will occur at this time.

**FIRST POWER-ON:** when the 2 V threshold is reached, the node turns on for the first time and communicates with the gateway to signal its presence in the system. The gateway replies with an acknowledgment. The MCU then programs the RTC to wake the node up after a scheduled time. The RTC puts the node in an ultra-low-power sleep mode by removing power supply to the MCU and its peripherals.

**SLEEP MODE:** in ultra-low power sleep mode, only the RTC is on (55 nA current consumption), together with the power management section which keeps charging the storage element.

**ACTIVE MODE:** when the RTC awakes the node, the MCU starts the acquisition of accelerometer data, performs some statistical analysis (for simplicity we limit ourselves to minimum, maximum and average on the three axes in this example) on a 0.5 second window and sends data to the gateway. Transmission parameters for the LoRa radio are spreading factor 5, bandwidth 1625 kHz, code rate 4/5. The node goes back to sleep mode till the RTC awakes it again.

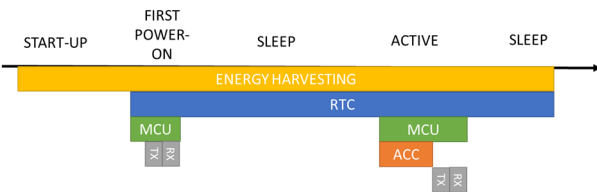


Fig. 6. Operational modes of the node, colours show which components are active in the different phases.

Fig. 7 depicts the main components of the power management section. The output of the rectifier is fed to a buck-boost DC/DC converter (Texas Instruments bq25570) specifically designed for harvesting energy from low voltage, low power sources (down to 100 mV and 15  $\mu$ W). Given the limited amount of energy that can be harvested (down to few tens of  $\mu$ W), the storage elements need to present ultra-low leakage currents. Typical leakage of rechargeable batteries, supercapacitors and ceramic capacitors are not compatible with the requirements of the application. To overcome this issue, the storage element comprises two 470  $\mu$ F ultra-low-leakage tantalum capacitors from AVX (TMJE447K), capable of limiting leakage to less than 2  $\mu$ A.

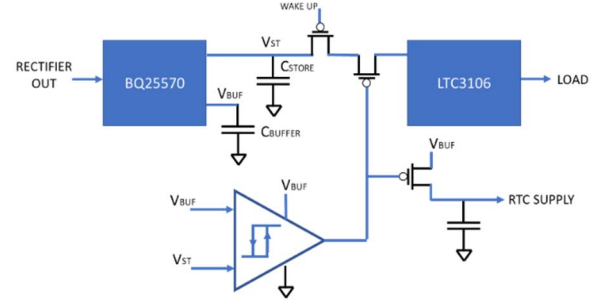


Fig. 7. Scheme of the power management section of the wireless sensor node.

Given the application, the node is expected to be unable to receive any type of input power when the vehicle is turned off. Therefore, the capacitors will be likely completely discharged when the vehicle is started. The main issue affecting such a scenario is that the bq25570 operates in a very low efficiency (less than 10%) mode till it exits cold-start voltage of around 2 V, which means that charging a fully depleted capacitance of around 1 mF with input power of few tens of  $\mu$ W up to 2 V will require times in the order of 10-20 minutes to exit START-UP mode.

In order to overcome this problem, the converter directly charges only a 22  $\mu$ F capacitor ( $C_{\text{BUFFER}}$ , blue line in Fig. 8). When  $V_{\text{BUF}}$  reaches 3.6 V, a buck DC/DC converter in the bq25570 is turned on briefly, transferring charge from  $C_{\text{BUFFER}}$  to  $C_{\text{STORE}}$ , whose voltage (green curve in Fig. 8) will slightly increase, till  $V_{\text{BUF}}$  goes back at 2 V and the buck DC/DC converter gets turned off. The procedure then starts again without the harvester re-entering cold-start and reducing the time required to exit cold-start at the beginning of operation ( $\sim$  42 times). The maximum charge voltage of  $C_{\text{STORE}}$  is 3.3 V.

Power supply to the node is then provided through a Linear Technology LTC3106 buck-boost DC/DC converter which is connected to the energy storage capacitors. It is capable of operating down to 700 mV, allowing the node to be operational with  $C_{\text{STORE}}$  voltages between 0.7 and 3.3 V, corresponding to 4.8 mJ of available energy. The RTC controls switching between low-power sleep and active mode by turning on or off the LTC3106 through a PMOS switch.

An additional series switch is inserted to allow for operation of an undervoltage lockout circuit which prevents the supplies of the LTC3106 and the AB1805 to be below the minimum required levels. In this case, the current



consumption of the two ICs would be too high to allow for charging of the capacitor. Since no fixed voltage is available on the node to determine an absolute threshold, as shown in Fig. 7, an ultra-low power comparator based on Texas Instruments TLV3691 compares the voltage on  $C_{\text{BUFFER}}$  and  $C_{\text{STORE}}$ , allowing first power on only when  $V_{\text{ST}}$  reaches 95% of  $V_{\text{BUF}}$ . A large hysteresis is inserted to avoid the node to turn off again as soon as the  $C_{\text{STORE}}$  discharges during normal operation.

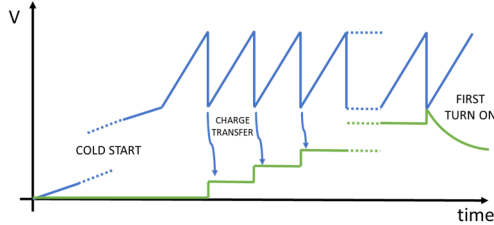


Fig. 8. Mechanism to efficiently manage charging of a fully depleted storage capacitance.

### III. MEASURED PERFORMANCE OF THE WPT SYSTEM

A measurement campaign has been conducted in a realistic scenario, adopting the car engine compartment to monitor the charge time of the storage capacitors, located on the top layer of the node, for several node locations and distances from the RF powering station. Two RF sources at 2.45 GHz, providing an EIRP (Effective Isotropic Radiated Power) of 27 dBm to comply with regulations, have been adopted for the present situation. The expected storage energy into the two tantalum capacitors is 5.12 mJ, widely sufficient for the LoRa operation. In LOS (Line-of-sight) conditions, this WPT system is able to rectify 230, 70 and 27  $\mu\text{W}$  at 30, 60 and 90 cm, respectively.

For demonstrative purposes, ten positions of the wireless sensor nodes have been chosen for temperature and acceleration monitoring. During the measurements, a maximum distance of 54 cm between the tag and the closer RF source has been considered, enabling all the key parts of the engine compartment to be monitored. It is worth mentioning that in this case, the sensors are placed in a metallic environment widely affected by reflections and in NLOS (Non-line-of-sight) propagation conditions.

In Table 1, the results achieved in terms of recharge time and rectified power are summarized.

Table 1. Charging time, average power at the rectifier output, and distance from the nearest RF source for ten sensors placed in different compartment sectors of a car engine.

Monitored Part	Charge Time	Mean $P_{\text{out}}$ at the Rectifier	RF Source Min. Distance
Battery	44 s	240 $\mu\text{W}$	28 cm
Engine Head	8 s	1320 $\mu\text{W}$	20 cm
Water Pump	68 s	155.3 $\mu\text{W}$	34 cm
Engine Support	127 s	83.1 $\mu\text{W}$	42 cm
Radiator	79 s	133.7 $\mu\text{W}$	39 cm
Air Filter	173 s	61 $\mu\text{W}$	20 cm
Hydraulic Oil Tank	191 s	55.3 $\mu\text{W}$	36 cm
Fuse Box	62 s	170.3 $\mu\text{W}$	36 cm
Radiator Fan	259 s	40.8 $\mu\text{W}$	54 cm
Pump Drive Belt	92 s	114.8 $\mu\text{W}$	42 cm

The average efficiency of the LTC3106 is between 80 and 85%, depending on the input voltage, which is further reduced to about 70% due to inefficiencies in power-on of the LTC3106 and charging of the decoupling capacitors on the MCU and peripherals. This leads to 1.7 mJ to be drawn from  $C_{\text{STORE}}$  on every active mode cycle, well below the energy that can be stored on the node.

Detailed energy requirements from the node components to operate during the active mode cycle are presented in Table 2.

Table 2. Components and corresponding energy demand.

Component	Required Energy
MCU	360 $\mu\text{J}$
Accelerometer	270 $\mu\text{J}$
LoRa Transceiver	415 $\mu\text{J}$
RTC	13.2 $\mu\text{J}$

The obtained node charging times are consistent with a monitoring system schedule of data communication every five minutes, which is perfectly reasonable for the targeted application.

### IV. CONCLUSION

In this work, the design of a novel battery-less node, exploiting the LoRa protocol in the 2.4 GHz Band, has been demonstrated to be successfully operated in complex metallic environments, such as those related to automotive applications. The design and tests of the node have been provided and have shown robustness with respect to the ambient and the energy requirements.

A measurement campaign was conducted in a real engine compartment scenario, and demonstrated the effectiveness of the whole WPT system, with capacitors charging times adequate for the requirements of the proposed monitoring system for automotive applications.

### REFERENCES

- [1] W. J. Fleming, "New Automotive Sensors—A Review," *IEEE Sensors Journal*, vol. 8, no. 11, pp. 1900-1921, Nov. 2008.
- [2] K. Zannas, H. E. Matbouly, Y. Duroc and S. Tedjini, "Flipping a Coin, Heads or Tails. Flipping an RFID Tag on Metal, ETSI or FCC Bands," in *Proc. 2019 IEEE MTT-S International Microwave Symposium (IMS)*, Boston, MA, USA, 2019, pp. 283-285.
- [3] L. Ukkonen, L. Sydanheimo, and M. Kivikoski, "Effects of Metallic Plate Size on the Performance of Microstrip Patch-Type Tag Antennas for Passive RFID," *IEEE Antennas and Wireless Propagation Lett.*, vol. 4, pp. 410-413, 2005.
- [4] A. Sharma, A. T. Hoang, F. Nekoogar, F. U. Dowla, and M. S. Reynolds, "An Electrically Small, 16.7 m Range, ISO18000-6C UHF RFID Tag for Industrial Radiation Sources," *IEEE Journal of Radio Frequency Identification*, vol. 2, no. 2, pp. 49-54, June 2018.
- [5] J. Grosinger, W. Pachler, and W. Bosch, "Tag Size Matters: Miniaturized RFID Tags to Connect Smart Objects to the Internet," *IEEE Microwave Magazine*, vol. 19, no. 6, pp. 101-111, Sept.-Oct. 2018.
- [6] N. Shinohara, H. Goto, T. Mitani, H. Dosho, and M. Mizuno, "Experimental study on sensors in a car engine compartment driven by microwave power transfer," in *Proc. 2015 9th European Conference on Antennas and Propagation (EuCAP)*, Lisbon, 2015, pp. 1-4.